OPTIMIZATION OF HETEROGENEOUS FENTON AND PHOTO FENTON REACTIONS FOR THE TREATMENT OF PALM OIL MILL EFFLUENT USING RESPONSE SURFACE METHODOLOGY

SADIQ SANI

UNIVERSITI SAINS MALAYSIA

2022

OPTIMIZATION OF HETEROGENEOUS FENTON AND PHOTO FENTON REACTIONS FOR THE TREATMENT OF PALM OIL MILL EFFLUENT USING RESPONSE SURFACE METHODOLOGY

by

SADIQ SANI

Thesis submitted in fulfilment of the requirements
for the degree of
Doctor of Philosophy

August 2022

ACKNOWLEDGEMENT

All praises are due to Allah (SWT), the Lord of the worlds, Who favoured and bestowed me with the determination and strength to bring my PhD dissertation work to successful completion at the School of Chemical Sciences of the Universiti Sains Malaysia (USM). May the Peace and blessings of Allah (SWT) be upon His beloved Prophet and Messenger (SAW), his family, companions, and those who follow their righteous paths until the Day of Recompense.

First and foremost, I would express deep appreciation to my principal supervisor and the Dean of the School, Professor Rohana Adnan. She tirelessly supervised the thesis work with the keen focus necessary for recording academic success. Her thoughtful suggestions, support, and advice provide a well-defined direction towards making it a considerable achievement.

Secondly, I would like to recognise and acknowledge the school's staff body's various support services and gestures, especially the technical, administrative, and academic staff. Specifically, I would like to appreciate the staff's efforts at the School's Glass Blowing workshop in fabricating a photoreactor box used at the experimental stage of the work. I would also like to appreciate the astonishing, work-friendly and pleasing atmosphere enjoyed among colleagues in the school and the wider University community.

Thirdly, I would want to recognise and acknowledge the Academic Staff Training and Development (AST&D) Scheme of the Tertiary Education Trust Fund (TETFUND) of Nigeria for the scholarship award to pursue the PhD programme, as well as the management of the Federal University Dutsin-Ma (my employer) for the sponsorship nomination and support.

Finally, my deepest and most heartfelt gratitude goes to my beloved parents, my mother, Malama Salamatu and my father, Malam Muhammad Sani (Late), for their persistent and unrelenting efforts towards my upbringing, primarily supervised by the former. May Allah (SWT) continue to shower his mercies on them for their upbringing on me with fashion for lifelong knowledge-seeking, discipline, and honesty. I would also want to show my profound gratitude to my adorable spouse Mrs Halima Isah for her persistent patience, support, understanding, encouragement, and prayers to me throughout the 3-year journey. It is my great pleasure to mention my lovely wards Sadiq (Jnr), Halimatu (Jnr) and Muhammad (*Malaysia born*), who consistently serve as my fountain source of hope, happiness, and emotional energy for work towards building a brighter future that is beneficial for them.

Sadiq Sani
December 2021

TABLE OF CONTENTS

LIST OF TABLES

Page

LIST OF FIGURES

Page

LIST OF SYMBOLS

$\Delta G^{\ddagger}$	Gibbs free energy of activation
$\Delta H^{\ddagger}$	Enthalpy change of activation
$\Delta S^{\ddagger}$	Entropy change of activation
R_{sample}	Measured reflectance of a sample
$R_{standard}$	Measured reflectance of a standard
A	Heterogeneous catalyst dosage
a_o	crystal lattice constant
B	H_2O_2 concentration
C	Contact time or irradiation time
D	Dilution ratio
E	Initial pH of the slurry
E_g	Bandgap energy
eV	Electron volt
F	Agitation speed
Fe_i	Iron interstitial
G	Absorbent's absorption time
hν	Photon
k_0	Zero-order reaction rate constant (M s^{-1})
k_1	First-order reaction rate constant (s^{-1}),
k_2	Second-order reaction rate constant (M s^{-1})
O_i	Interstitial oxygen
R∞	Reflectance of specimen's infinite thickness
V_{Fe}	Iron vacancy
V_O	Oxygen vacancy
β	Full-width of the peak at half maximum (FWHM)

γ	Electronic transition constant
λ	Wavelength (nm)
$F(R_\infty)$	Kubelka–Munk function
K	Coefficient of absorption
S	Scattering coefficient
T	Temperature (K)
t	Reaction time
Fe^{3+}	Ferric ion
Fe^{2+}	Ferrous ion

LIST OF ABBREVIATIONS

ANOVA	Analysis of Variance
AOPs	Advanced Oxidation Processes
AT-POME	Anaerobically treated palm oil mill effluent
BBD	Box-Behnken design
BET	Brunauer-Emmett-Teller
BJH	Barrett-Joyner-Halenda
BOD	Biochemical Oxygen Demand
CCD	Central Composite Design
COD	Chemical Oxygen Demand (mg L^{-1})
COD_r	COD reduction (mg L^{-1})
D_{BET}	BET adsorption average pore-width
D'_{BET}	BET desorption average pore-width
D_{BJH}	BJH adsorption average pore width
D'_{BJH}	BJH desorption average pore width
DD	Doehlert design
DIW	Deionised water
DOE	Design of Experiment
D_{TEM}	Grain size
D_{TEM}	TEM mean particle size
DTG	Derivative Thermogravimetric Analysis
D_{XRD}	Crystallite size
D_{XRD}	XRD mean crystallite size
E_{COD}	COD reduction efficiency (%)
EDX	Energy Dispersive X-ray spectroscopy
E_{TOC}	TOC reduction efficiency (%)
Fe_3O_4 NPs	Magnetites nanoparticles
Fe_3O_4@C NCs	Carbon-encapsulated magnetite nanocomposites
FTIR	Fourier Transform Infrared Spectroscopy
F-value	Fisher's Value
H_2O_2	Hydrogen Peroxide
ICCD	International Centre for Diffraction Data

N/A	Not available
$^{\bullet}O_2H$	Hydroperoxyl radicals
$^{\bullet}OH$	Hydroxyl radical
OVAT	One-variable-at-a-time
pH	pH value
PL	Photoluminescent
POM	Palm Oil Mill
POME	Palm Oil Mill Effluent
PSD	Particle Size Distribution
RSM	Response Surface Methodology
RSS	Sum of squares for the residual errors
S_{BET}	BET surface area
S_{BJH}	BJH adsorption cumulative surface area of pores
S'_{BJH}	BJH desorption cumulative surface area of pores
SEM	Scanning Electron Microscopy
S_{Ext}	t-plot surface area
SE_{β}	Standard error of the coefficient
S_{Lang}	Langmuir surface area
TDS	Total dissolved solids
TEM	Transmission Electron Microscopy
TGA	Thermogravimetric Analysis
TOC	Total Organic Carbon (mg L^{-1})
TOC_r	TOC reduction (mg L^{-1})
TS	Total Solids (mg L^{-1})
TSS	Total Suspended Solids (mg L^{-1})
UV	Ultraviolet
V_{BET}	BET adsorption total pore volume
V'_{BET}	BET desorption total pore-volume
V_{BJH}	BJH adsorption total pore volume
V'_{BJH}	BJH desorption total pore volume
w/w	weight/weight (mg/mg)
XRD	X-ray diffraction

LIST OF APPENDICES

PENGOPTIMUM TINDAK BALAS FENTON DAN FOTO FENTON HETEROGEN BAGI RAWATAN EFLUEN KILANG KELAPA SAWIT MENGGUNAKAN KAEDAH RESPONS PERMUKAAN

ABSTRAK

Pembuangan efluen kilang kelapa sawit (POME) yang tidak dirawat mempunyai kesan buruk terhadap biota akuatik dan alam sekitar kerana kandungan permintaan oksigen kimia (COD) dan kandungan jumlah karbon organik (TOC) yang tinggi. Kajian ini telah menyiasat keberkesanan nanopartikel magnetit (Fe_3O_4 NPs) dan nanokomposit magnetit terkapsul karbon (Fe_3O_4@C NCs) sebagai pemangkin heterogen Fenton dan foto-Fenton untuk rawatan POME dikaji. Kaedah solvoterma dan hidroterma digunakan untuk mensintesis kedua-dua mangkin. Pemangkin dicirikan menggunakan pelbagai teknik dan digunakan untuk merawat POME melalui saringan satu langkah menggunakan reka bentuk Box-Behnken melalui kaedah respons permukaan yang melibatkan tujuh pemboleh ubah iaitu dos pemangkin, kepekatan H_2O_2, masa sentuhan penyinaran, tahap pencairan, pH POME, kelajuan pengadukan dan masa penyerapan. Reka bentuk tersebut melibatkan sebanyak 62 eksperimen dan empat pembolehubah bergerak balas ialah pengurangan TOC (TOC_r), kecekapan pengurangan TOC (E_{TOC}), pengurangan COD (COD_r) dan kecekapan pengurangan COD (E_{COD}). Model yang dibangunkan diperhalusi, diuji dengan analisis varians (ANOVA) dan disahkan menggunakan data eksperimen. Keupayaan guna semula pemangkin, kinetik dan termodinamik bagi rawatan POME dikaji. Keputusan ANOVA bagi rawatan Fenton menggunakan Fe_3O_4 NP menunjukkan model COD_r yang signifikan secara statistik ($F = 137.67$, $p = 0.00$) dengan ketepatan yang mencukupi (54.2) dan pekali variasi (4.7%) yang memuaskan. Nilai tindak balas yang

diramalkan bagi parameter optimum bagi dos pemangkin = 300 mg L^{-1}, kepekatan H_2O_2 = 408 mg L^{-1}, tahap pencairan = 0.0029, pH sluri = 3.0 dan masa penyerapan = 300 min berpadanan dengan nilai yang didapati secara eksperimen dengan nilai R^2 menghampiri 1 (0.9965).. Keputusan ANOVA dan pengoptimuman yang serupa dicatatkan bagi tindak balas Fenton dan foto Fenton menggunakan Fe_3O_4@C NCs. Degradasi POME menggunakan pemangkin Fe_3O_4 NPs mematuhi model kinetik tertib kedua untuk proses Fenton (R^2 = 98.6%, R^2-adj = 98.3%) sementara tindak balas foto Fenton mematuhi model kinetik jenis Elovich (R^2 = 99.8%, R^2-adj = 99.7%). Bagaimanapun, degradasi POME oleh Fe_3O_4@C NCs mematuhi model kinetik tertib dan model resapan intrapartikel Weber-Morris untuk proses Fenton (R^2 = 95.4%, R^2-adj = 94.2%) dan model Bingham untuk proses foto Fenton (R^2 = 99.7%, R^2-adj = 99.6 %). Semua tindak balas adalah tidak spontan ($\Delta G^{\ddagger}$ = 30-105 kJ mol^{-1}) dan endotermik ($\Delta H^{\ddagger}$ = 1.6-20.7 kJ mol^{-1} K^{-1}). Prestasi kitar semula menunjukkan bahawa kecekapan pengurangan COD Fe_3O_4 NPs menurun sehingga 52.6% melalui proses Fenton dan sehingga 83.1% melalui proses foto-Fenton setelah empat kitaran. Sementara itu, kecekapan pengurangan COD Fe_3O_4@C NCs pada akhir kitaran keempat adalah 22.4% dan 62.7% masing-masing melalui proses Fenton dan foto-Fenton. Walaupun penemuan yang dilaporkan ini adalah pada skala makmal, teknik ini sangat berpotensi untuk dikembangkan lebih jauh untuk aplikasi berskala besar.

OPTIMIZATION OF HETEROGENEOUS FENTON AND PHOTO FENTON REACTIONS FOR THE TREATMENT OF PALM OIL MILL EFFLUENT USING RESPONSE SURFACE METHODOLOGY

ABSTRACT

Disposal of untreated palm oil mill effluent (POME) has adverse effects on aquatic biota and the environment due to its high chemical oxygen demand (COD) and total organic carbon (TOC) content. This work investigated the effectiveness of magnetite nanoparticles (Fe_3O_4 NPs) and carbon-encapsulated magnetite nanocomposites (Fe_3O_4@C NCs) as heterogeneous Fenton and photo-Fenton catalysts for POME treatment. Solvothermal and hydrothermal methods were employed to synthesise the two catalysts. The catalysts were characterised using various techniques and the optimisation of the experimental parameters were investigated via a one-step screening using a Box-Behnken design via response surface methodology involving seven variables which are catalyst dosage, H_2O_2 concentration, contact/irradiation time, dilution ratio, pH of POME, agitation speed, and absorption time. Four response variables: TOC reduction (TOC_r), TOC reduction efficiency (E_{TOC}), COD reduction (COD_r) and COD reduction efficiency (E_{COD}) were evaluated and a total of 62 runs were considered. The models developed were refined, tested by analysis of variance (ANOVA) and validated using experimental data. The catalyst recyclability, kinetics and thermodynamics of POME removal were investigated. ANOVA for Fenton treatment on Fe_3O_4 NPs shows the refined COD_r model to be statistically significant (F = 137.67, p = 0.00) with favourable adequate precision (54.2) and coefficient of variation (4.7%). Predicted responses under optimum parameters of catalyst dosage = 300 mg L^{-1}, H_2O_2 concentration = 408 mg L^{-1}, dilution ratio = 0.0029, slurry pH = 3.0

and absorption time = 30.0 min agree with the experimentally validated values having the R^2 value close to unity (0.9965). Similar ANOVA and optimisation outcomes were recorded for Fenton treatment on Fe_3O_4@C NCs and photo-Fenton treatment on both catalysts. Degradation of POME using Fe_3O_4 NPs catalyst follows second-order model for Fenton process (R^2 = 98.6%, R^2-adj = 98.3%) while the photo-Fenton reaction are best described by the Elovich-type model (R^2 = 99.8%, R^2-adj = 99.7%). On the hand, the degradation of POME using Fe_3O_4@C NCs follows the Weber-Morris intraparticle diffusion model for the Fenton process (R^2 = 95.4%, R^2-adj = 94.2%) and Bingham model for photo-Fenton process (R^2 = 99.7%, R^2-adj = 99.6%). Similar trends were observed for mineralisation kinetics of both catalysts. All reactions were non-spontaneous ($\Delta G^{\ddagger}$ = 30-105 kJ mol^{-1}) and endothermic ($\Delta H^{\ddagger}$ = 1.6-20.7 kJ mol^{-1} K^{-1}). The recyclability performance shows that the COD reduction efficiency of Fe_3O_4 NPs was reduced to 52.6% in the Fenton process and to 83.1% in the photo-Fenton process after four cycles. Meanwhile, the COD reduction efficiency of Fe_3O_4@C NCs was reduced to as much as 22.4% and 62.7% in the Fenton and photo-Fenton process, respectively. Although the findings are currently at a laboratory scale, the current technique is highly potential to be developed further for large-scale applications.

CHAPTER 1
INTRODUCTION

1.1 Background of Study

Supply of safe and high-quality water is one of the global challenges of the twenty-first century but essential for the sustenance of industries and supporting the living of multitudinous humans and other animate on earth. A very meagre amount of water is available for industrial and domestic applications, although the hydrosphere occupies the most significant fraction of the earth surface, 71% (Kim & Lee, 2022). The bulk of the water resources' mass constitutes the oceans (97.5%) and freshwater (2.5%) with most of it (1.7%) locked in directly inaccessible form for consumption as glaciers, permanent snow cover at poles and in mountaneous regions (DellaSala, 2018). The remaining proportion accessible for use is made up of liquid freshwater (0.8%) distributed in the atmosphere (as water vapour), as ground water, lakes, and rivers (DellaSala, 2018). The supplies of accessible water resources for direct industrial and domestic utilisation are inherently scarce.

Moreover, freshwater quality varies depending on its chemical, microbial, and physical compositions, which natural phenomena and anthropogenic processes influence. Throughout the third world countries, the inadequacy of sanitary facilities and unhygienic practices are ubiquitous, leading to the degradation of water quality and human life occasioned by retrogressive political, economic, and climatic influences (World Bank, 2017). Globally, around 4.0 billion people have been reported to be currently suffering from water shortages with approximately half of them facing water scarcity (Filho *et al.*, 2022). A loss of ~US$1.101 trillion per annum is recorded due to the absence of essential water and sanitation based on the 2020 global GDP of US$84.71 trillion (UNICEF & WHO, 2020). In recent decades, the upsurge in

population density and steady rise in anthropogenic industrialisation witnessed throughout the globe resulted in high daily freshwater demands for industrial and domestic activities. Uncoordinated discharge of untreated effluents resulting from such activities escalated the scourge of widespread pollution, causing a significant imbalance beyond the tolerable composition in the environment through the release of persistent organic and inorganic substances into the atmosphere, land, and freshwater aquifers (Chaturvedi *et al.*, 2020).

Environmental pollution from industries has contributed immensely to reducing water quality and causing detrimental effects to all forms of life, including humans, animals, and plants (Mo *et al.*, 2018). Recently, much attention is being devoted to research on releasing partially-treated or untreated effluents from agroindustries such as olive oil mills, wineries, food processing, beverages industries, etc. into the environment. Palm oil mills (POMs) are among the most critical agroindustrial sectors with considerable contributions to the Malaysian economy. However, they generate large amounts of wastes that are highly potential for environmental pollution.

1.2 Statement of Problem

Release of untreated, partially- or biologically treated POME from palm oil mills (POMs) or palm oil refineries (PORs) into adjacent water bodies has detrimental influences on the sustainability of the ecosystem, aquatic biota, and humanity due to high recalcitrant pollutant content, with potential toxicity. It may lead to eutrophication and impact photosynthesis adversely and cause toxicity in aquatic flora and fauna (Chan *et al.*, 2010; Vijayaraghavan *et al.*, 2007; Zainuri *et al.*, 2018b). POMs and PORs subject raw POME to a series of temporal treatments in the ponding system

(clarifier tank, acidic cooling, anaerobic, aeration, facultative, and polishing ponds) for a retention time of more than 3-4 months before being discharged into the surrounding rivers. Both raw POME and biologically treated POME (BT-POME) samples contain high levels of COD (~10,000 mg L^{-1}), TSS and colour intensity far beyond the typical discharge standards even after several cycles of biological treatments (Aris *et al.*, 2008; Parthasarathy *et al.*, 2016; Taha & Ibrahim, 2014b). The ponding and conventional techniques of POME treatment are grossly inadequate in degrading/mineralising the recalcitrant pollutants content in the effluent. Thus, effective effluent treatment methods such as advanced oxidation processes (AOPs) need to be secured to overcome these challenges before POME discharge into natural water bodies. Homogeneous ambient Fenton and photo-Fenton AOPs have been adjudged to be simple, independent, and efficient for removing pollutants in POME and other wastewaters either at pretreatment, primary or secondary stage of treatment (Dewil *et al.*, 2017; Gamaralalage *et al.*, 2019). However, Generation of a large volume of ferric hydroxide sludge due to the inability for Fe^{2+} catalyst regeneration, excessive consumption of Fenton's reagent (Fe^{2+}/H_2O_2), narrow range of reaction pH and additional costs of treating the generated sludge before disposal into adjacent water bodies, among other drawbacks, are the inherent disadvantages that limit their application in POME treatment.

These concerns can be addressed using suitable low-cost solid catalysts, such as synthetic Fe_3O_4 NPs and Fe_3O_4@C NCs, as substitute to homogeneous ones in heterogeneous Fenton and visible light-assisted photo-Fenton. The catalysts are designed to be sufficiently stable to leaching under severe oxidant and acidic conditions; magnetically separable from the reaction medium after treatment; and recyclable during a set of repeated treatments. Kinetics and thermodynamics

performances of the processes in POME pollutant degradation/mineralisation have also been evaluated. It should also possess high activity for pollutants removal, allows only marginal leaching of active cations, be stable over a wide range of reaction pH and temperatures, and high hydrogen peroxide conversion with minimal decomposition.

1.3 Objectives of Research

The objectives of this research are:

1. To synthesize and characterise magnetite nanoparticles (Fe_3O_4 NPs) and carbon-incapsulated magnetite nanocomposites (Fe_3O_4@C NCs);
2. To study the effects of operational parameters (e.g. catalyst dosage, H_2O_2 concentration, contact/irradiation time, dilution ratio, initial slurry pH, agitation speed, and absorbent's absorption time) on the COD and TOC reductions (COD_r, TOC_r) and reduction efficiencies (E_{COD}, E_{TOC}) of the catalyst; to determine the optimised response factors and condition for degradation and mineralisation of pollutants in POME during the heterogeneous Fenton and photo-Fenton treatment based on a one-step Box-Behnken Design (BBD) type of Response Surface Methodology (RSM); and
3. To study the thermodynamics, kinetics, and the recyclability of the Fe_3O_4 NPs and Fe_3O_4@C NCs catalysts in the degradation and mineralisation of pollutants in POME by the heterogeneous Fenton and photo-Fenton catalysis.

1.4 Novelty of Research

The novelty of this work lies in its effort to address the treatment of POME using heterogeneous, magnetically recoverable, Fenton and visible-light-driven photo-Fenton catalysts fabricated based on magnetite nanoparticles (Fe_3O_4 NPs) alone and in associated form as carbonised glucose-encapsulated magnetite nanocomposite (Fe_3O_4@C NCs).

1.5 Research Scope

The scope of this thesis is limited to the fabrication of heterogeneous Fenton catalysts for application in POME treatment from a palm oil mill in Pulau Pinang, Malaysia, under the absence and influence of simulated visible light irradiation. The efficiency of the treatment is limited only to the measurement of the COD and TOC values of the POME. The parameters (catalyst dosage, H_2O_2 concentration, etc.) on which the processes depend upon were screened in a series of experiments based on a one-step Box-Behnken Design (BBD) response surface methodology (RSM) for optimisation and validation of the responses (degradation, mineralisation, and their efficiencies). The reusability of the catalysts in the effluent treatment was evaluated by conducting a series of a fixed number of experimental runs utilising recycled aliquots of the catalysts, monitoring their degradation and mineralisation efficiencies for each cycle, and assessing the overall performances throughout the recycling process. Kinetics and thermodynamics modelling of the effluent mineralisation and degradation processes by the catalysts also were explored.

1.6 Dissertation Structure

This PhD dissertation is comprised of seven (7) chapters. The first chapter, Chapter One, discusses the background developments and perspectives of palm oil production in the palm oil industry, focusing on extraction processes, national economic growth, pollutant waste generation, regulatory standards for POME discharge, and conventional POME treatment technologies. Advanced oxidation processes, emphasising heterogeneous Fenton and photo-Fenton processes, were briefly introduced as alternative techniques to their conventional counterparts for POME treatment. This chapter also states the research problem, objectives, research questions, and hypotheses.

Chapter Two is the Literature Review, which highlights outcomes from the literature relevant to Fenton and photo-Fenton processes with specific attention to POME treatment. It also presents works on similar forms of agro-industrial wastewater, treatment conditions, treatment efficiencies, advantages, and disadvantages for using homogeneous and heterogeneous.

Chapter Three lists and describes all the materials, experimental and statistical methods employed in this work. Meanwhile, Chapter Four presents the results on the characterisation of the magnetic NPs and NCs. The results of the Fenton and photo-Fenton treatments of POME on the two types of the catalysts based on the BBD response surface methodology performed in the dissertation work are presented in Chapter Five. The evaluation and the discussions of the catalyst's overall performance in the degradation and mineralisation of pollutants in POME via the Fenton and photo-Fenton heterogeneous processes are presented in this Chapter Six. Chapter Seven states all the conclusions, highlight the important findings of the work and puts forward some recommendations for future work.

CHAPTER 2
LITERATURE REVIEW

2.1 Overview of the oil palm agroindustry

Oil palm represents one of the most versatile crops in tropical regions, especially Malaysia and Indonesia. The palm genus *Elaeis* (Greek for 'oil') consists of two different species: *Elaeis guineensis*, originally from West Africa, and *Elaeis oleifera* (oil-producing), originally from Central and South America (Abu Bakar *et al.*, 2018). Both palm species are well known as highly efficient oil-producing plants, similar to rapeseed, sunflower, cottonseed and soybean plants (Hussin *et al.*, 2022). The industry is the leading agroindustries contributing enormously to the country's income, with oil palm plantations accounting for 77% of agricultural land and approximately 15% of the total land area estimated at 15.9 million hectares (Rahman *et al.*, 2021; Su *et al.*, 2022). The average crude palm oil (CPO) production in the agroindustry grew significantly from less than 100,000 tonnes in 1960 to about 19.14 million tonnes in 2020 (Haryati *et al.*, 2022; Nambiappan *et al.*, 2018). Based on Figure 2.1, palm oil production superseded soybean oil from just 13.6% in 1990 to 33% of total oil and fats production in 2015. This disparity is because oil palm has a higher annual oil yield per hectare than other oilseeds crops, including soybean (Chin *et al.*, 2013). Other countries contributing to palm oil production include Thailand, Columbia, Nigeria, and Indonesia. Indonesia and Malaysia are the two top palm oil producers and produce 85% of the world's palm oil (Ziaei & Ali, 2021). Malaysia is currently the second-largest producer and exporter of palm oil globally with crude palm oil (CPO) production 19.14 million tonnes and the total export of palm products amounting to 26.59 million tonnes in 2020 (Haryati *et al.*, 2022; Parveez *et al.*, 2021). Figure 2.1 compares the global production of oils and fats in 1990 and 2020.

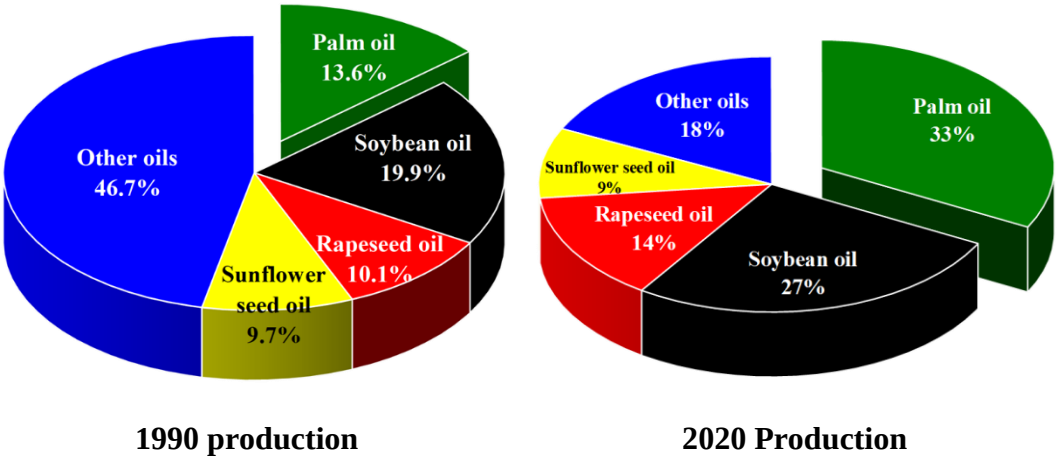

Figure 2.1 World oil and fat production in 1990 (Ahmad *et al.*, 2003) and 2020 (Forum For the Future., 2021)

While crude palm oil production decreased by 3.6% to 19.14 million tonnes in 2020, foreign exchange earnings from palm oil and oil palm products export have increased by 8.5% to RM 73.25 billion in the same year compared to the previous year records (Parveez *et al.*, 2021). Oil palm plantation acreage has slumped to 5.87 million hectares in 2020 compared to 5.90 million hectares recorded in the previous year (Parveez *et al.*, 2021). Malaysia was the world's largest crude palm oil producer before Indonesia outperformed in 2006 and slipped to the second position (Bruno, 2021). Table 2.1 summarise the performances of the Malaysian palm oil industry.

Table 2.1 Performance of the Malaysian oil palm industry in palm oil production between 2009 to 2017

Marketing Year	Palm oil production performance indices						Reference
	PA[a]	CPOP[b]	POE[c]	OPPTE[d]	POER[e]	OPPER[f]	
2009	4.69	17.56	15.88	22.43	36.95	49.66	MPOB (2010)
2010	4.85	16.99	16.66	23.06	44.86	59.77	MPOB (2011)
2011	5.00	18.91	17.99	24.27	60.47	80.41	MPOB (2012)
2012	5.08	18.79	17.56	24.56	52.96	71.40	MPOB (2013)
2013	5.23	19.22	18.15	25.70	45.27	61.36	MPOB (2014)
2014	5.39	19.67	17.31	25.07	44.50	63.62	MPOB (2015)
2015	5.64	19.96	17.45	25.37	41.26	60.17	MPOB (2016)
2016	5.74	17.32	16.05	23.29	43.34	64.59	MPOB (2017)
2017	5.81	19.92	10.56	23.97	46.12	77.85	MPOB (2018)
2018	5.85	19.52	16.49	24.88	38.66	67.52	MPOB (2020)
2019	5.90	19.86	18.47	27.88	38.03	64.84	MPOB (2020)

a. PA: *planted acreage*; b. CPOP: *crude palm oil production (Million tonnes)*; c. POE: *palm oil exports (Million tonnes)*;
d. OPPTE: *oil palm products total exports (Million tonnes)*; e. POER: *palm oil exports revenue (Million tonnes)*;
f. OPPER: *oil palm products export revenue (Billion RM)*

Oils that fall into the category of vegetable oil comprises soybeans oils/other oilseeds oils (≈55% global production), palm oil (≈35% of global production), coconut oil, cottonseed oil and palm kernel oil (OECD/FAO, 2018). Table 2.2 summarise the future projections of the Malaysian palm oil industry.

Table 2.2 Projections on global production of palm oil as vegetable oils (OECD/FAO, 2018)

Marketing year	Global vegetable oils production (million tonnes)	The proportion of palm oil from vegetable oil production		Average price (USD/tonne)
		Production (Million tonnes)	*Production (%)*	
2015-2017	190	65.1	34.3	784
2018	202	71.1	35.2	829
2019	206	72.6	35.3	829
2020	210	74.2	35.4	830
2021	214	75.8	35.5	834
2022	217	77.1	35.5	843
2023	221	78.4	35.5	853
2024	224	79.6	35.5	863
2025	228	80.8	35.5	875
2026	231	82.0	35.5	883
2027	235	83.2	35.5	892

2.1.1 Palm oil extraction as an environmental pollution source

Several stages are involved in crude palm oil (CPO) extraction from fresh fruit bunches (FFBs). The first is sterilisation, where FFBs just brought in the mill are subjected to high-pressure steam (120 - 140 °C at 40 psi)(Liew *et al.*, 2015). The next stage is stripping, in which the sterilised fruits are separated from the bunch stalks via a rotary drum thresher (Wu *et al.*, 2010). The detached fruits then undergo the stripper's bar screen. A bucket conveyor collects the screened fruits and channels them into a digester with a central rotating shaft equipped with mechanical arms fitted to a steam-heated cylindrical vessel that softens and mashes the fruits. The shaft rotation coupled with temperatures of 80 - 90 °C loosens the nut's outer covering (mesocarp). The nuts' CPO is squeezed out using a mechanical press machine (Igwe & Onyegbado, 2007; Wu *et al.*, 2010). The press machine gives out a mix of highly viscous fluids (fibrous material, debris, insoluble solids, palm oil, and water) that must be clarified. Therefore, the oil emulsion is first broken into two phases – lighter oil droplets flow through the watery mixture to the top while the emulsion settles to the bottom of the clarifier – by

adding hot water as a barrier. The clarifier's bottom phase is the sludge, and the POME is drained off and purified before being discharged (Rupani *et al.*, 2010). Other significant waste materials are also generated because of the oil extraction process, as shown in Figure 2.2.

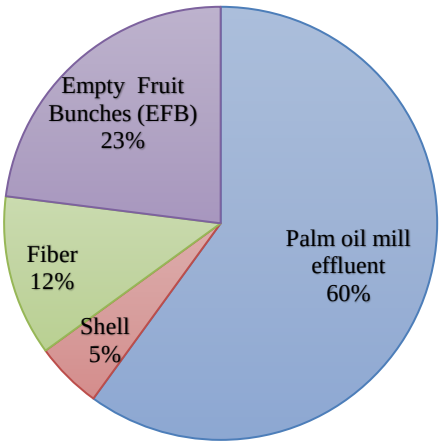

Figure 2.2 Waste produced from the palm oil mill per tonne of FFBs (Bala *et al.*, 2014b)

For every tonne of FFBs in the mill, the waste can be divided into 23% EFBs,12% mesocarp fibre, 5% shell and 60% POME (Baharuddin *et al.*, 2010; Bala *et al.*, 2014a, 2014b). Based on Figure 2.2, POME represents most of the waste from the palm oil industry. During the wet extraction of palm oil, copious quantities of water of about 1.5 m^3 are consumed per tonne of FFBs processed (Azmi *et al.*, 2012). Of an estimated 5.0-7.5 tonnes of water consumed during the wet extraction process of FFBs per tonne of crude palm oil produced, more than 2.5-3.75 tonnes are converted into POME, a significant drawback to the industry (Bello *et al.*, 2013; Gamaralalage *et al.*, 2019; Parthasarathy *et al.*, 2016; Wu *et al.*, 2009). Lorestani (2006) found that FFBS sterilisation, CPO extraction and clarification, and kernel and shell separation of cracked mixtures in the hydrocyclone were the processes that generated the most POME at 36%, 60%, and 4%, respectively. A rapid increase in POMs from 355 mills

(Chin *et al.*, 2013) to 457 mills (Parveez *et al.*, 2021) further exacerbated this problem. Figure 2.3 shows a flow diagram that simplifies the palm oil production process.

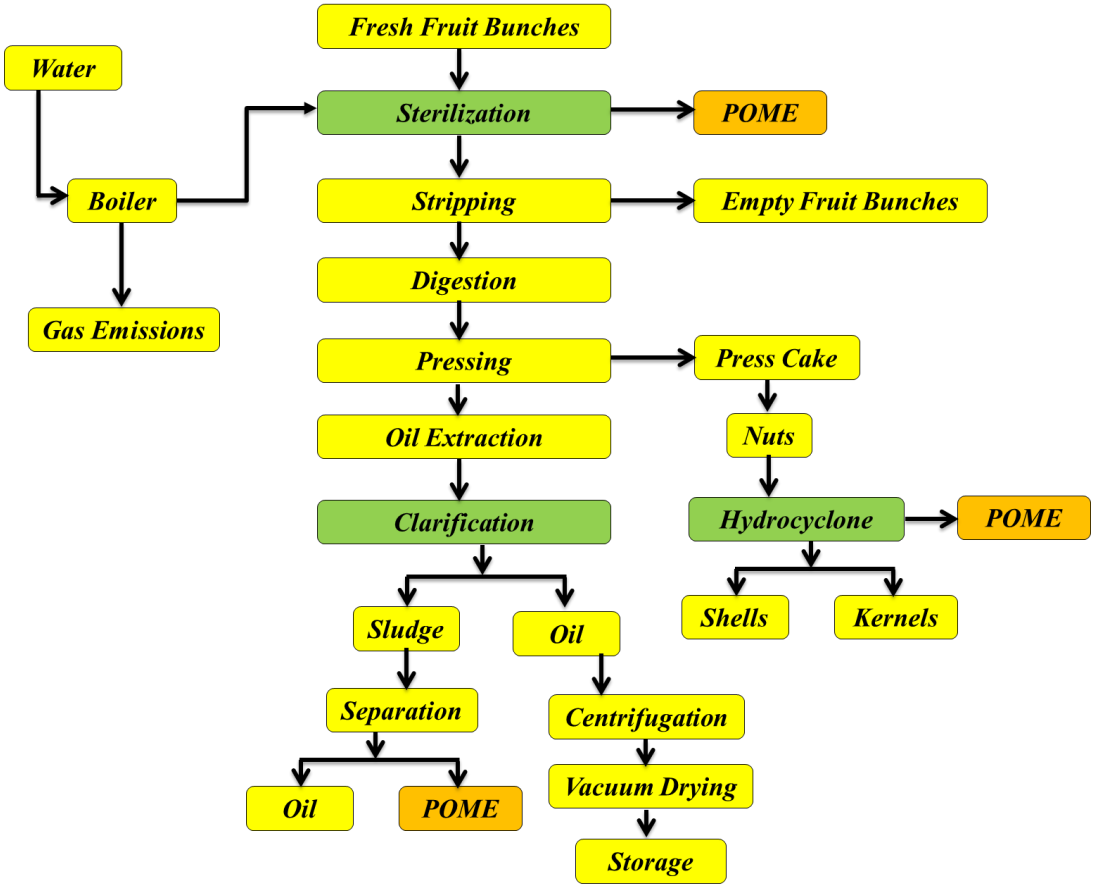

Figure 2.3 Diagram of the palm oil mill processes (Igwe & Onyegbado, 2007; Rupani *et al.*, 2010)

Raw or fresh POME is a thick brownish liquid mixture of 95–96% water, 4–5% total solids, 0.6–0.7% oil/grease with high chemical oxygen demand (COD) and biochemical oxygen demand (BOD) values (Poh *et al.*, 2010). About half to four-fifths of the total solids are suspended solids, mainly constituting palm fruit mesocarp debris generated by steriliser condensate, separator sludge and hydrocyclone process (Bello *et al.*, 2013; Parthasarathy *et al.*, 2016; Wu *et al.*, 2009).

Moreover, as POME has high acidity and solids, it cannot be directly discharged into the waterway. Liew *et al.* (2015) highlighted that the massive

quantities of POME generated from most of the water output of crude palm oil processing, if not properly managed, will pollute the waterways near the POMs. Table 2.3 lists the typical characteristics of raw POME. Raw POME has high temperatures (80-90 ^{o}C), and the effluent is rich in organic contaminants such as lignin (4700 ppm), phenolics (5800 ppm), pectin (3400 ppm) and carotene (8 ppm) (Zainuri *et al.*, 2018a). The industry has generated a large volume of waste annually, which kept threatening the ecological environment's sustainability (Zainuri *et al.*, 2018a).

Table 2.3 Characteristics of raw POME (Mohammad *et al.*, 2021a)

Parameter	**Range (mg L^{-1})**
Chemical oxygen demand (COD)	15,000–100,000
Biochemical oxygen demand (BOD)	10,250–43,750
Total suspended solids (TSS)	5000–54,000
Ammoniacal nitrogen (NH_3-N)	4–80
Oil and grease	130–18,000
Total nitrogen (TN)	180–1400
pH	3.4–5.2

Malaysia's oil palm industry has become a considerable investment due to the steady expansion and beneficial returns witnessed over the years. Despite the immense contributions to the Malaysian economy and improved living standards among citizens of this country, the oil palm industry has also been recognised as a significant contributory source of the highest pollution loadings being discharged into local canals and rivers (Bala *et al.*, 2015; Wu *et al.*, 2009; Zainuri *et al.*, 2018a). However, as the massive production expands, an even larger volume of palm oil mill effluent (POME) is produced. POME contains soluble materials that are harmful to the environment, either in the form of soluble gases such as methane (CH_4), sulphur dioxide (SO_2) and ammonia (NH_3), soluble liquids or solids, with concentrations above the threshold limit values (Igwe & Onyegbado, 2007). When discharged into receiving water bodies, the untreated effluent could cause significant environmental problems due to its very

high BOD, COD (Santana *et al.*, 2019), oil and grease, total solids (TS) and total suspended solids (TSS) (Parthasarathy *et al.*, 2016; Wu *et al.*, 2009). While water pollution originating from this practice has continued to be a subject of public complaints, reports on histopathological changes in fish organs exposed to POME attested to the effluent's probable toxicity to humans (Bello *et al.*, 2013; Gamaralalage *et al.*, 2019).

2.1.2 Regulatory frameworks for effluent discharge limits

Several regulatory and legislative frameworks have been enforced to ensure environmental protection and safety against untreated POME ills and other agro-industrial wastewaters discharged into the environment. For example, the Environmental Quality Act (EQA) of 1974 promulgated the Environmental Quality Order and Environmental Quality Regulations of 1977, granting legal jurisdiction to the Malaysian Department of Environment (DOE) for enforcement and compliance (Azmi *et al.*, 2012; Zainuri *et al.*, 2018a). The DOE set the minimum standard characteristics and discharge limit of POME, compared with those provided by the World Health Organization (WHO) and the United States Environmental Protection Agency (USEPA), as illustrated in Table 2.4. Therefore, strict compliance with these legislations is necessary to ensure environmental sustainability through wastewater reclamation and recycling for domestic and industrial uses (Azmi *et al.*, 2012).

Table 2.4 POME standard discharge limits (Ahmad *et al.*, 2006; Ahmad Shahrifun *et al.*, 2015; Department of Environment, 2009; Madaki and Seng, 2013; USEPA, 2000; WHO, 1971)

Parameters	**POME standard discharge limits**			
	DOE[a]	*EQA*	*USEPA*	*WHO* [e]
BOD_5	50[b]	100	–	–
COD (mg L^{-1})	1000	1000[c]	NR[d]	
Total solids (mg L^{-1})	1500	1500[c]	–	500–1500
Suspended solids (mg L^{-1})	400	400	–	–
Oil and grease (mg L^{-1})	50	50	0.3	–
Ammoniacal nitrogen (m g L^{-1})	100	150[c]	NR	–
Total nitrogen (mg L^{-1})	200	200[c]	-	–
pH	5.0	5.0 – 9.0	6.5 – 8.5	6.5 – 9.2
Temperature (°C)	45	45	–	–

a. The Malaysian DOE discharge limits have been in effect from 1986 onwards
b. DOE has stipulated no new value since 1982
c. Stringent standards in environmentally sensitive areas of Sabah and Sarawak, Malaysia starting 2006
d. Parameter not required (NR) under USEPA guideline for POME discharge
e. WHO acceptable standard guideline values for drinking-water

2.1.3 Contemporary POME treatment technologies

Consequently, the POME treatment to the highest degree possible before discharge into the environment is a legal imposition POMs in Malaysia need to obey. The POMs are usually overwhelmed by difficulties in handling and treatment of large volumes of POME generated. The inability of a more significant number of POMs to comply with the law led to their consistent failure in meeting the stringent discharge limits legally imposed by the authorities. Instead of upgrading to the more efficient treatment technologies available, most POMs (85%) use the open ponding system that works on the principle of suspended growth-activated sludge (Mohammad *et al.*, 2021b). The relatively low capital, cheaper operational and maintenance costs of the system might justify its wholesale adoption by the POMs. However, ponding facilities cannot comprehensively degrade the harmful organic pollutants in POME (Zainal *et al.*, 2017). They employ anaerobic ponds that could require a large expanse of land (~30-45 acres) to store POME for extended hydraulic retention times (~3 months) to

satisfactorily degrade the effluent before discharge into water bodies (Wang *et al.*, 2015). POME degradation by anaerobic bacterial digestion releases enormous amounts of biogas. An estimated 50% of POMs in Malaysia have effluent treatment plants that cannot capture biogas emissions. The emissions are eventually released into the atmosphere, contributing to the greenhouse effect exacerbating global warming. The need to upgrade the currently deployed obsolete technology has been adversely affected by faulty regulatory enforcement and seasonal and milling-related fluctuations in POME composition and properties (Abdulsalam *et al.*, 2018).

Many alternative physicochemical treatments (evaporation, superficial skimming, coagulation, adsorption, membrane filtration, etc.) and biological technologies have been proposed for the conventional treatment of POME (Zhang *et al.*, 2008). Laboratory-scale high-rate anaerobic bioreactors developed for POME treatment include up-flow anaerobic sludge blanket (UASB) reactor (Fang *et al.*, 2011), up-flow anaerobic filtration (Borja & Banks, 1994), up-flow anaerobic sludge blanket-hollow centred packed bed (UASB-HCPB) reactor (Poh & Chong, 2014), fluidised bed reactor (Borja & Banks, 1995) and up-flow anaerobic sludge fixed-film (UASFF) reactor (Zinatizadeh *et al.*, 2007). Others that have also been studied for POME treatment are anaerobic contact digester and continuously stirred tank reactor (CSTR) (Choorit & Wisarnwan, 2007). Only a few of these approaches have been deployed for full-scale operations due to their unsatisfactory performances, high capital investment and high maintenance costs (Zhang *et al.*, 2008). Although many works have also been carried out on the treatment of POME using advanced oxidation processes (AOPs) such as the conventional homogeneous Fenton processes, the bulk of the literature is still scarce on the utilisation of heterogeneous Fenton or photo-

Fenton processes for POME treatment with only a few pieces of reported works available.

The classical Fenton reaction is restricted by a narrow pH range of 2-4 (Bello *et al.*, 2019). Thus, setting up the treatment pH at values exceeding the upper limit of 4.0 enhances the sequential oxidation and quick precipitation of Fe(II) into Fe(III), which abruptly results in the eventual termination of the Fenton process (Wang *et al.*, 2012).

Table 2.5 enumerates the variety of available Fenton processes. A heterogeneous Fenton treatment utilising solid catalysts based on iron oxides to extend the pH range, prevent the precipitation of Fe(II) ions out of the solution and reduce the formation of iron (III) sludge is required. Although Fe(III) can initiate a Fenton-like reaction at a prolonged rate, the process is sustained by the improved Fe(II) ion regeneration through ionic recycling of the Fe(II)/Fe(III) redox couple. Hyphenating the process with photochemical or electrochemical measures accelerate the further regeneration of Fe(II) ions in the heterogeneous treatment systems is desired in the Fenton-based reaction. Photo-Fenton solid catalysts based on iron oxides can accelerate the recycling of iron species in the Fe(II)/Fe(III) redox couple, which eventually enhances the efficiency of the POME treatment. The heterogeneous Fenton and photo-Fenton processes proposed in this work are among the effective AOPs that promise POME treatment due to their demonstrated process economy and high efficiency in treating similar effluents (Barrera-Salgado et al., 2016; Wang et al., 2012).

Table 2.5 Configurational variations of Fenton processes (Wang *et al.*, 2012)

Process variant	Fenton reagents	pH range	Remarks
Classical Fenton	H_2O_2, Fe(II) ion	2–4	It requires activation source but involves loss of iron catalysts
Fenton-like	H_2O_2, Fe(III) ion	2–4	It needs no activation source but Involves loss of iron catalysts
Classical electro-Fenton	Electrolytically generated H_2O_2, Fe(II) ions; H_2O_2, electrolytically generated Fe(II) ions	2–4	It needs electrochemical activation and involves loss of iron catalysts
Classical photo-Fenton	H_2O_2, Fe(III) complex, Fe(II) ions	Acidic to neutral	It requires light activation and involves loss of iron catalysts
Heterogeneous Fenton	H_2O_2, solid catalyst based on iron oxide	Wide range	It involves neither activation source nor loss of iron catalysts
Heterogeneous Photo-Fenton	H_2O_2, solid catalyst based on iron oxide	Wide range	It requires light activation and involves no loss of iron catalysts
Heterogeneous Photoelectro-Fenton	Electrolytically generated H_2O_2, solid catalyst based on iron oxide	Wide range	It requires both light and electrochemical activation and involves no loss of iron catalysts

2.2 Conventional Treatment Methods

POME treatments using various conventional methods, including biological and physicochemical techniques, have been reported. In principle, traditional wastewater treatment employs several physical, chemical, and biological techniques to remove contaminants, such as soluble or colloidal substances, organic or inorganic matter, nutrients, or pollutants (metals, organics, etc.) from the effluent. POME treatment by biological techniques such as aerobic activated sludge reactor (Vijayaraghavan *et al.*, 2007) has been reported. Many other studies reported such treatments utilising physicochemical techniques, including membrane technology, coagulation-flocculation, and evaporation methods (Hassan *et al.*, 2002). Few workers

have reported POME treatment using the emerging advanced oxidation process technologies such as Fenton oxidation (Bello & Raman, 2017), and photo-Fenton oxidation (Kanakaraju *et al.*, 2017). Table 2.6 summarises the efficiencies of some studies carried out on the POME treatment.

The pale-yellow colour (λ = 400-700 nm) of POME for discharge – which is a shade of the initial brownish colour – that remains even after the conventional ponding, biological, coagulation-flocculation treatments signifies the presence of recalcitrant pollutants (Bello *et al.*, 2013; Soleimaninanadegani & Manshad, 2014; Zainuri *et al.*, 2018a). Continued colour accumulation in the receiving water bodies could shield sunlight penetration from reaching underneath, paralysing photosynthetic activities in the aquatic environment (Kant, 2012). In addition, chelation of metal ions by some high-affinity chemical pollutants in POME may occur, leading to exposure of aquatic biota to the toxicity of the resulting hazardous complex products.

Table 2.6 Summary of technologies for POME treatment

Technology	Process description	Removal efficiency	Reference
Adsorption techniques			
Steam activated bio-adsorbent from oil palm biomass	A 200 g of sliced oil palm fronds (OPF) were pyrolyzed at 500 ± 5 °C for 2 h prior to cooling to 38 °C for 2 h at 100 cm^3 min^{-1} steam flow rate. The cooled biochar was milled for 10 min into a fine slurry, filtered through a sieve with 250μm and 74μm mesh sizes to obtain granular biochar retentate and micro-fine biochar as filtrate. Finally, both biochar samples were oven-dried for 48 h at 105 °C and stored in separate sealed polypropylene vessels. Finally, batch adsorption experiments were performed on weighed amounts of biochar samples (0- 0.75 g) in 25 mL samples of unfiltered and filtered POME. The mixtures were shaken at 150 rpm and 30°C ambient temperatures for 24 h. At equilibrium, each sample mixture was filtered through a 0.45μm syringe filter and analysed for residual COD concentrations and colour intensities.	COD (81%) Colour (96%)	Lawal *et al.* (2020)
Activated carbon prepared from palm kernel shell (PKSAC)	Batch adsorption uptake was studied at various initial concentrations of lignin in POME (0.505-5.05 kg m^{-3}), adsorbent weight (100mg), optimum contact time (120h), temperature (300K).	Lignin adsorption capacity (60-490g kg^{-1})	Boontham *et al.* (2022)
Electrocoagulation and coagulation processes			
Electrocoagulation on in-situ aluminium (III) hydroxide ($Al(OH)_3$) coagulant with hydrogen peroxide as an oxidising agent	The electrocoagulation process was carried out in a 10 L polypropylene container as a reactor, accommodated with 8 L of POME sample. both electrodes, an anode and cathode, were made up of aluminium and were connected vertically with 40 mm gap apart. Each electrode is 200 mm x 150 mm x and 5 mm in dimension with active surface area of 1.131×10^{-1} m^2. electrocoagulation reactor was operated for 8 h optimal time.	COD (97%) BOD (92%)	Mohamad *et al.* (2022)

Table 2.6 (Continued)

Technology	Process description	Removal efficiency	Reference
Coagulation–flocculation using plant materials fenugreek as a coagulant with okra and Aloe vera as the flocculants	Coagulation-flocculation experiments using standard jar tests were employed to determine the influence of optimum parameters such as effluent initial pH (4), coagulant dosage (22.24 g/L) and flocculant dosage (16.77 mL/L) for fenugreek-okra and effluent initial pH (4), coagulant dosage (24.13 g/L) and flocculant dosage (20 mL/L) on the removal efficiencies of the coagulant-flocculant samples optimized with Response Surface Methodology (RSM).	On fenugreek-okra TSS (88.19%), TUR (78.35%) COD (30.56%) On fenugreek-*Aloe vera* TSS (83.40%) TUR (82.78%) COD (32.95%)	Lim *et al.* (2021)
Coagulation with magnetic *Moringa oleifera* (MMO) using Response surface methodology	Coagulation experiments using standard jar tests were employed to determine the effect of the optimum parameters weight percent (wt%) of magnetic nanoparticles (1.0 wt%), sonication time (2.35 min) and sonication temperature (50 °C) on the coagulation performance parameters TSS, COD and sludge volume index (SVI) removals and fabricate an efficient MMO coagulant.	TSS (83.3%) Colour (28.1%) COD (85.2%) SVI (485 mL/g)	Mohamed *et al.* (2022)
Advanced oxidation processes			
Fenton oxidation	Batch Fenton oxidation modelled experiments were performed on diluted POME (non-filtered) in a pair set involving an open system for liquid samples analyses and a closed flask system for gaseous samples analyses.	NH_3-N (73%), TOC (91%), TN (11%), TP (99.9%).	Gamaralalage *et al.* (2019)
UV/TiO_2 and UV/ZnO photocatalytic systems	Both TiO_2 and ZnO photocatalysts were calcined at 573 K and stored in amber glass sampling bottles. After photoreaction, photocatalysts were filtered, washed multiple times with water and ethanol, and then recycled.	COD (74.1% on ZnO; 80% on TiO2)	Ng *et al.* (2017)
Filtration technique			
Calcined limestone horizontal roughing filter	First Phase: The limestone was crushed into three different sizes (mm), washed, and dried. Second phase: The limestone was calcined at 800 ºC and used as horizontal roughing filters in column studies with three different flow rates.	COD (51%)	Dashti *et al.* (2019)

Pollutant and pigments in POME are non-biodegradable, making conventional treatments insufficient and inefficient for POME degradation and mineralisation (Bello *et al.,* 2013; Wu *et al.,* 2009). Detailed cost analysis revealed that the conventional POME treatment systems, such as ponding, are prone to further environmental pollution and have the lowest utilisation of renewable resources without significant profits (Wu *et al.,* 2009). The benefits and drawbacks of various individual strategies reported in the literature are described in Table 2.7.

The utilisation of these conventional techniques is disadvantaged for having long retention time, slow start-up reactors, large land area requirement for digesters, high energy consumption, a lower rate of pathogen inactivation, membrane short-life/fouling and high operational costs (Poh & Chong, 2009). Furthermore, replacing or reinforcing the existing conventional treatment techniques becomes necessary to ensure effective degradation and mineralisation of POME pollutants (Bello *et al.,* 2013). Therefore, this warrants an alternative method that should be economical, energy-efficient, and environmentally friendly and, above all, must be sustainable. One such method with strongly merited potential as an advanced oxidation process (AOP) is oxidation over heterogeneous Fenton or photo-Fenton catalysts.

2.3 Advanced Oxidation Processes

Multiple research efforts are currently being made in developing inexpensive and more effective methods for treating raw POME (Gamaralalage *et al.,* 2019). The efforts are to ensure complete compliance with the existing stringent environmental regulations. Wastewater treatment using advanced oxidation processes (AOPs) is based on the generation of highly reactive and non-selective radicals as powerful oxidants (Huang *et al.,* 1993). The term referred to oxidation processes capable of rendering

water treatment at ambient temperature and pressure by generating an adequate amount of hydroxyl radicals as originally defined by (Glaze *et al.*, 1987).

Table 2.7 Advantages and disadvantages of conventional methods for POME treatment (Abdurahman *et al.*, 2011; Crini & Lichtfouse, 2019)

Technique	Advantages	Disadvantages
Aerobic digestion		
	a) It has a shorter hydraulic retention time than anaerobic digestion b) It is highly efficient in handling toxic wastes	a) It requires high energy due to aeration b) Its sludge has a lower rate of pathogen inactivation than anaerobic sludge c) It is unsuitable for land use as fertilizer
Anaerobic digestion		
	a) It has low energy requirements due to the absence of aeration b) It produces methane gas as a valuable end-product c) It generates sludge that could be used for land applications as fertilizer	a) It has a longer hydraulic retention time the aerobic digestion b) It requires a large expanse of land area for digesters c) It has slow start-up reactors (granulating reactors)
Membrane filtration		
	a) It consistently produces treated water of good quality b) It requires smaller space for membrane treatment plants c) It is capable of disinfecting water	a) Its membrane has a short life b) Its membrane suffers from fouling c) It is more expensive than some other conventional methods
Evaporation technique		
	a) Its solid residues can be used as a raw material supply for the manufacture of fertilizer b) Evaporators have various configurations with established energy costs to suit a purpose c) Versatile in recycling water distillates for rinsing operations	a) It involves the consumption of a high amount of energy b) Unbearable high costs of investments for medium- and small-scale industries c) Its High load of effluent concentrates may pose secondary pollution risks d) Its Concentrates may corrode evaporator heating elements and incur additional costs for replacement
Adsorption processes		
	a) Technologically simple process design and adaptable to many treatment formats b) Wide range of available adsorbent materials c) Global and selective elimination of target contaminants d) Highly efficient treatment with fast kinetics and high-quality treated effluent e) It has a low capital cost requirement	a) The relatively high cost of commercially activated carbons b) Generation of a high amount of sludge poses risks for secondary pollution c) Increased costs for handling and disposal of generated sludge d) Large variability in performances among adsorbent materials e) Increased costs for chemical derivatization of materials to improve efficiency f) Increased costs for regeneration due to rapid saturation, clogging and losses of materials g) Cost-inefficient and non-viable for certain industrial applications

In the past two decades, AOPs have received great attention as alternative methods for the reduction of the organic load in different kinds of wastewaters generated from different processing agro-industries such as olive oil mills (Alver *et al.*, 2015; Michael *et al.*, 2014), winery (Amor *et al.*, 2019; Souza *et al.*, 2013) and POMs (Aris *et al.*, 2008; Bashir *et al.*, 2017; Bello & Raman, 2017). AOPs can transform non-biodegradable pollutants into nontoxic, biodegradable substances by oxidizing a broad range of organic pollutants quickly and non-selectively by generating very reactive species such as hydroxyl radical (•OH) (Mohajeri *et al.*, 2010; Salari *et al.*, 2009). Oxidation by H_2O_2 alone has been found ineffective for high concentrations of certain refractory contaminants because of low reaction rates at reasonable H_2O_2 concentrations. The utilisation of ozonation AOPs, for example, could have the disadvantage of forming bromate ion species, a strong carcinogen, as a by-product during the treatment of bromide-containing effluent (Baus *et al.*, 2005). Transition metal salts (e.g. iron salts), ozone and UV-light, can activate H_2O_2 to form •OH (Shu *et al.*, 2006). AOPs have currently evolved to include, among other methods, photocatalysis (Cheng *et al.*, 2017; Ng & Cheng, 2017), ozonation/UV at elevated pH's (Wu *et al.*, 2018), ozonation/hydrogen peroxide (Qiang *et al.*, 2010), ozonation@Catalysts (Dai *et al.*, 2014), ozonation/activated carbon (Wang *et al.*, 2019), ultrasound-assisted oxidation (Manickam *et al.*, 2014), microwave-assisted oxidation (Garcia-Costa *et al.*, 2019), wet air oxidation (Palas *et al.*, 2018), per-sulphate oxidation (Vicente *et al.*, 2011), and Fenton oxidation processes (Saleh & Taufik, 2019). Among AOPs, photo-Fenton processes using both homogeneous and heterogeneous catalysts have been investigated to be a cheaper and more effective alternative for treating palm oil mill effluent. The homogeneous Fenton process has particularly attracted great interest given its high capacity to generate •OH through the